

Computer vision methods for anomaly removal

M. Peura

Finnish Meteorological Institute, Development Branch, P.O. Box 503, 00101 Helsinki, Finland

Abstract. We present a set of techniques designed for detection and removal of the anomalies appearing in weather radar imagery. Methodologically, the emphasis is on computer-vision related techniques, hence deviating from the current mainstream of the techniques based on if-then rules and/or auxiliary meteorological data sources.

Our main focus is on sea clutter (ships, waves) and interfering external emitters (telecommunication, other radars). In addition, we present tools for detecting the sun, birds, insects, and aircraft.

As a core component, the applied techniques involve recognition of graphical primitives (size, elongation, orientation, and steepness). Information on these primitives is then combined in order to detect higher-level objects.

Another central feature is to treat detection and removal as distinct processes. This design is a natural choice if detection products are desired for each phenomenon separately. Second, the results of detection are cumulatively stored as a probabilistic anomaly map, hence a continuum of radar images can be generated by varying a single threshold parameter. High thresholds imply products in which only the most evident anomalies have been cut off (or marked) whereas low thresholds imply products in which the most of the anomalies and, as a compromise, some precipitation, have been removed.

In this paper, we explain and illustrate the computer vision techniques applied at the Finnish Meteorological Institute. Related software has been in operational use since May 2002.

1 Introduction

Weather radar images are frequently contaminated by non-meteorological echoes as well as echoes caused by anomalous propagation. Some anomalies are shown in Fig. 1.

Automated detection of the various anomalies has proven to be a difficult task. However, even if the performance of an

Table 1. Detectors and their primary targets.

Detector	Target
BIOMET	birds and insects near the radar
SPECK	noise; distinct specks
EMITTER	line segments
SUN	long line segments
SHIP	ships (and aircraft)
VERT_GRAD*	sea waves and ducting effects
METEOSAT*	suspiciously warm data
DOPPLER*	non-continuous doppler data

* under development; not operational

automated detection scheme remains inferior to the quality of a meteorologist’s analysis, there are still advantages like speed, consistency, and objectivity. One should also keep in mind that the requirement for the purity of data differs among applications. For example, operational generation of warnings often requires conservative anomaly removal, if any, whereas in computing motion vectors pure radar data samples are preferred even at the cost of spatial coverage.

Practically, our computer vision based approach means that the targets are treated above all by their visual appearance. Consequently, we group and discuss targets primarily under the detection algorithms expected to work on them. For example, small specks originate from various sources, but a filter that removes them all in a single pass will do. However, in many cases, similar appearance tends to refer to similar origins. The detector set developed at the FMI is shown in Table 1.

In the filtering process, we treat detection and removal as separate processes. This principle is motivated by two aspects of efficient end-product computation. First, some anomalies are of interest of certain customer groups, such as birds for aviation. Second, products have varying requirements for the purity of data. Hence, the results of detection are presented as images of continuous-valued probabilities, enabling several products to be generated from a single orig-

Correspondence to: M. Peura (Markus.Peura@fmi.fi)

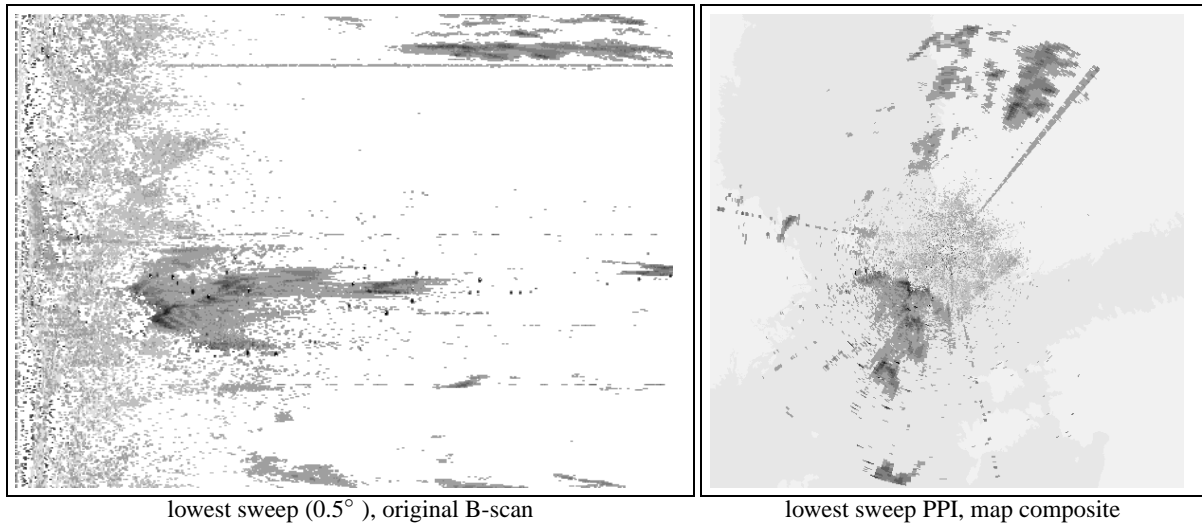


Fig. 1. An example of radar data containing several types of anomalies – FMI Korppoo radar at 04:30 EET on 9 July, 2002. The only actual precipitation is in the North / North-East. The anomalies are speckle noise, sun (the continuous line segment pointing to 40°), emitter (170° & 280°), insects (near the radar), ships (sharp small specks; sidelobes), and sea clutter (large speck between 180° and 270°). The detectors presented in this paper will be demonstrated using this data.

inal by repeated thresholding.

In the following section, we list some elementary image analysis techniques that serve as building blocks for our actual algorithm presented in Sec. 3 and Sec. 4. The obtained results are discussed in Sec. 5.

2 Elementary image analysis tools

2.1 Mask operations

A variety of digital image processing tasks can be performed by means of *masks* (also called windows or templates). The basic idea is to consider the neighborhood of each pixel, compute a function on it, and store the value in the result image.

The operator applying this neighborhood, that is, the mask, can be linear or nonlinear. Probably the most common nonlinear mask operator is the *median filter* which means computing the midmost value in the histogram of the mask. Median filter is used for cancelling sharp details such as outliers (say, ships in radar imagery) and speckle noise.

2.2 Morphological operations

In computer vision, *morphology* refers to operations causing expansion or retraction of shapes, typically not as a result of geometrical scaling but by so called *erosion* and *dilation* of shapes (Haralick et al., 1987; Songa et al., 1993). Morphology can be used in separating and combining neighboring segments.

Erosion and dilation can be obtained for example by generalizing a median filtering such that instead of taking the center value, the median, one takes the n th value from the bot-

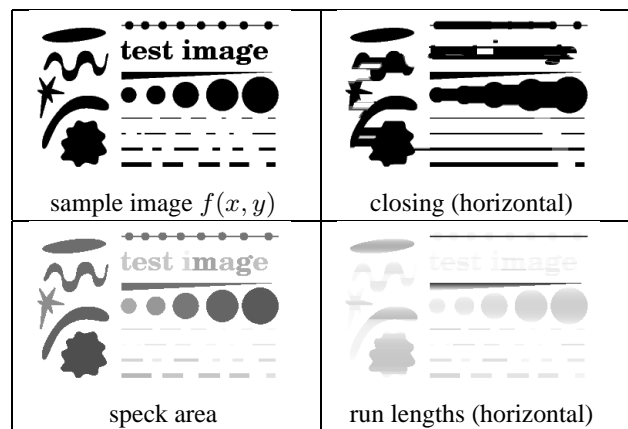


Fig. 2. Basic image analysis operators.

tom of the histogram for erosion and from the top for dilation. Performing erosion followed by dilation results in *opening* shapes; vice versa for *closing*. If the masks are rectangular, computation can be accelerated by pipeline design. Elongated masks yield directionally weighted results (Fig. 2).

2.3 Segment operations

Many graphics programs apply the *flood-fill* algorithm in painting objects automatically: “if this pixel is inside the area, and if it is not painted yet, paint it and restart this for the neighboring pixels”.

This technique can be also used in spreading information in an image. One may for example scan all each segment in the image, compute its area (closed curve integral), and then spread the result within the segment. An example is

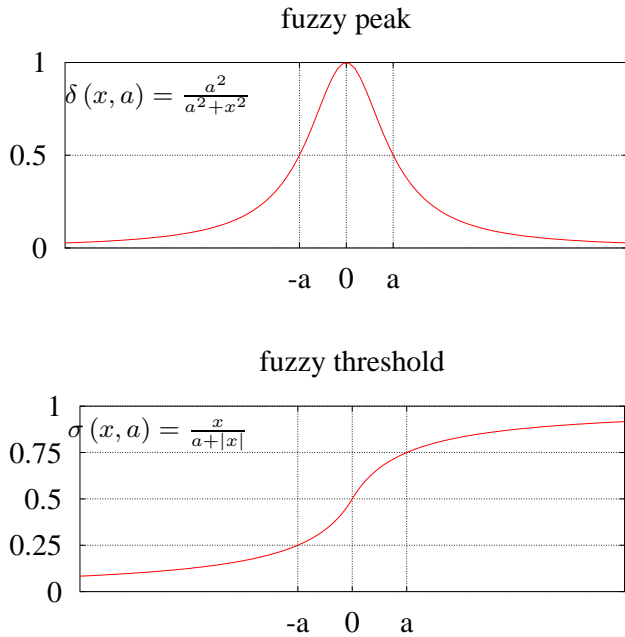


Fig. 3. Suggestions of simple fuzzy functions. In both functions, a is a steepness parameter referring to a “half-width”.

shown in Fig. 2. This way, further processing, say filtering too small specks in radar images, can be performed simply by thresholding and masking. Further shape descriptors can be found for example in (Peura et al., 1998).

The flood-fill is a memory-consuming operation but can be optimized by circularly dead-ending recursion.

If the objects of interest are elongated, it is reasonable to distinguish them by their run-lengths, that is, by the segment lengths calculated in either horizontal or vertical direction. Run lengths are easily computed by first accumulating lengths and then spreading the obtained lengths in the opposite direction.

2.4 Fuzzification

Targets appearing in meteorological radar data — different modes of precipitation, bright bands, sky conditions and anomalies — cannot be separated by applying strict dBZ thresholds. Hence, in detecting and classifying these targets we suggest producing smooth curves of probability (or certainty, confidence, quality, or Bayesian belief) instead of absolute if-then results. This approach also helps in keeping results independent from scaling and measuring units.

We propose using soft peak and threshold functions for communicating meteorologist’s expertise (Fig. 3). For motivation, consider translating the following sentence to a mathematical form: “if the size of the image segment is around 8 pixels, or at least between 4 and 12 pixels, and its maximal intensity is over 40dBZ, then it is probably a ship.”

3 Detection

3.1 BIOMET — birds and insects

In the Finnish radar network, birds and insects appear regularly from spring to autumn. These “biometeors” form widespread, low-intensity speckled patterns near the radar. Although their behaviour can be modelled to some extent (for birds, see Koistinen, 2000), designing a fully automatic detector is an ambitious project. Consequently, such detector seems to be not yet available but we introduce here a simpler pre-detector which extracts evidence of *possible* locations of biometeors. Nevertheless the current detector can be used in removing evident biometeors.

The basic idea is to assume that biometeor echoes remain under certain dBZ limit f' and remain under certain altitude h' . The detector can be formulated as $\text{BIOMET}(x, y) =$

$$\sigma(f' - f(x, y), \Delta f) \cdot \sigma(h' - h(x, y), \Delta h),$$

where x and y are coordinates in a B-scan image (hence synonyms for beam direction ϕ and radius r), and Δh and Δf are the expected half-width intervals. Applying $f' = -5\text{dBZ}$ with $\Delta f = 10\text{dBZ}$ as well as $h' = 2500\text{m}$ with $\Delta h = 500\text{m}$, the detection results for the data of Fig. 1 is shown in Fig. 6.

3.2 SPECK — speckle noise and distinct specks

Applying the segment methods (Sec. 2.3), detection of distinct specks is straightforward. One simply sets a threshold for the segment size (in pixels, i.e. bins) corresponding to the 50% probability of anomaly, then computes the segment sizes. We set this limit to $\Delta s = 12\text{pix}$, and obtain results shown in Fig. 6. It should be pointed out that median filtering is usually applied in this task, but its disadvantage is that it distorts all details, whereas SPECK picks up specks “by hand” and thus enables creating a separate detection image.

3.3 EMITTER and SUN — line segments

In the Finnish radar network, the most frequent type of interfering radiation appears as straight line segments cause by other emitters. However, due to geometry, distant precipitation may appear more or less similarly. The challenge is to distinguish between these two.

Our hypotheses are: 1) emitter anomaly appears as horizontal segments of length at least a pixels, 2) such segments have maximal vertical width of w pixels (=degrees), and 3) occurrence of short, beam-wise segments implies increased probability of larger emitter anomalies in that direction.

The SUN detector resembles the EMITTER with the exception that target segments are allowed to be thicker and the beam-wise confidence (Fig. 4, center) contains only the pre-computed peak in the direction of the sun. Otherwise the processing and results are very similar, hence not elaborated here.

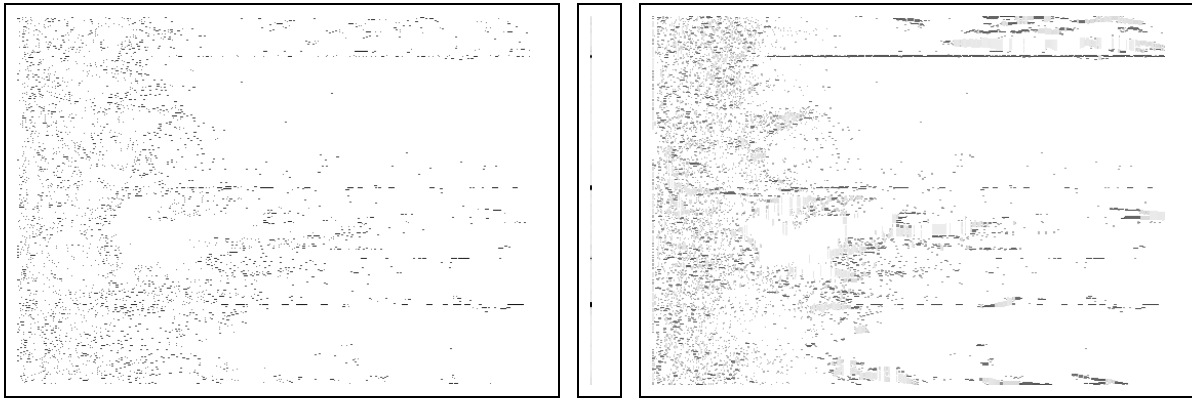


Fig. 4. Intermediate processing steps in detecting emitter segments with EMITTER (compare this with the b-scan image of Fig. 1). From left to right: 1) segments of vertical width 1° and the respective 2) thresholded averages of each beam, and 3) horizontal run lengths *from which vertical run lengths have been subtracted*.

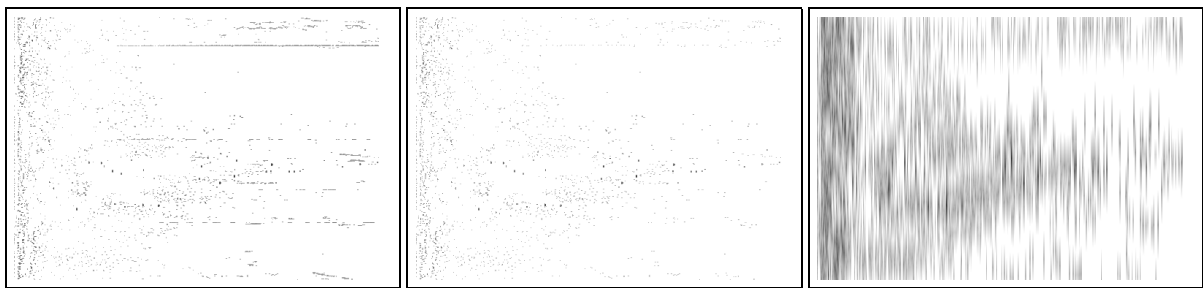


Fig. 5. Intermediate processing steps of SHIP. Left to right: 1) suspicious pixels extracted by simple high-boost filtering, 2) the previous result with horizontal segments pruned, and 3) artificially generated sidelobes to be matched with the actual ones in the input image.

3.4 SHIP — marine (and airborne) vessels

As ships and aeroplanes are efficient reflectors of electromagnetic radiation, that they appear as sharp spots in weather radar images. The challenge is to distinguish these spots from small convective cells; otherwise they risk being interpreted and forecasted as local showers or hail. Ships interfere even when they lie a couple of degrees off the radar beam; the strength of ship echoes makes them somewhat insensitive to vertical gradient based recognition. On the other hand, the spots have often sidelobes perpendicular to the radar beam, which helps in detection.

The SHIP detector is currently the computationally heaviest anomaly detector applied at the FMI. The processing time for one radar volume remains still below a few seconds on the current Pentiums.

The main strategy is to detect small but intensive separate spots. If sidelobes are neighboring the spots, they become detected, too. There is no space to explain the SHIP in detail, but some processing stages are shown in Fig. 5 and the results in Fig. 6.

3.5 VERT_GRAD, METEOSAT and DOPPLER — sea clutter detectors under construction

In spring, the temperature differences between sea and the lowest atmosphere causes radar beams to bend downwards, yielding strong echoes from sea waves and ships as well as

other anomalies like second trip echoes and external emitters. Hence, this problem appears especially in our coastal radars (Korppoo and Vantaa).

VERT_GRAD. Typically, sea clutter interferes the lowest sweep(s) and disappears relatively sharply on the upper sweeps. On the contrary, precipitation echoes have smoother vertical gradients. Hence, our strategy is to consider the vertical gradient which is, however, fuzzily weighted by its altitude; the weight is inversely proportional to altitude. In addition, we should somehow cancel already-passed positive gradients, hence we always compute the gradient from the minimum dBZ value obtained that far. We used 50%-limits 3500m for altitude and $-10\text{dBZ}/1000\text{m}$ for vertical gradient, and obtained the results shown in Fig. 6.

METEOSAT. Precipitation implies ice particles. Because of the low resolution currently available in the latitudes of Finland, the temperature of the smallest specks in radar images cannot be verified. Hence, we mask them out as a pre-processing stage. The results in Fig. 6 were obtained with a 50%-confidence threshold -5°C ; respectively 0°C for a 75%-confidence.

DOPPLER. As opposite to precipitation, some anomalies have inconsistent doppler velocity fields. Especially insects, dense flocks of birds as well as some sea anomalies appear as discontinuities in doppler data. The results in Fig. 6 were obtained by detecting continuities in a 3×3 pix window.

	detector response (b-scan)	extracted anomalies	filtered image
BIOMET			
SPECK			
EMITTER			
SHIP			
VERT_GRAD			
METEOSAT			
DOPPLER			

Fig. 6. Detection results for the case shown in Fig. 1.

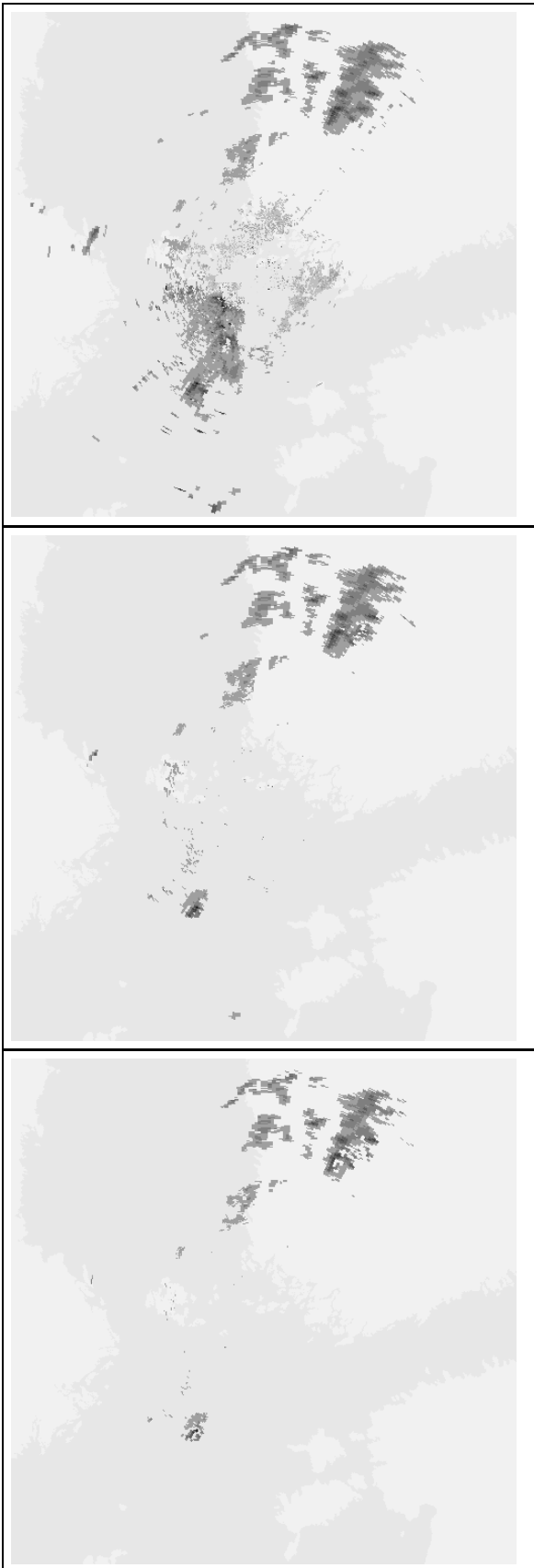


Fig. 7. Collective application of all the listed detectors with 75%, 50% and 40% filtering thresholds.

4 Removal

Typically, it is desired that the anomalies detected in a radar image should not be only marked as warnings for the end-user but also removed. However, it not obvious how the anomalous pixel intensities should be replaced. The default choice is to just cut them off, as we have done for the sample image (Fig. 1) in the filtered result images of Fig. 6. This policy should be however questioned if anomalies and precipitation are mixed. We suggest spreading the data from the neighboring, non-anomalous pixels by means of median-type filtering; elongated anomalies require perpendicularly elongated filters.

Finally, in Fig. 7 we show the original image from which all the detectors listed in this paper have been applied. Varying the filtering threshold illustrates how a user can achieve a desired POD/FAR-type compromise.

5 Discussion

We presented a set of anomaly detectors for weather radar images. The detectors share a common basis in a set of image analysis techniques, but otherwise the detectors vary in performance and computational complexity.

The performance of most detectors, especially for EMITTER, SUN and SHIP is satisfactory. Also the simple BIOMET works well in detecting the *existence* of birds and insects. The currently missing detector for strong bird echoes might be realized in the future based on the currently available “biometeor support field”. SPECK provides an exact means for handling individual specks – a property not achieved when using standard median filtering. Some detectors, like the METEOSAT, seem promising, but however do not seem to solve their proposed detection tasks autonomously but hopefully with a help of some additional information available in the future.

Acknowledgement. Thanks to J. Koistinen and H. Hohti for guidance, ideas and cooperation.

References

- Haralick, R. M., Sternberg, S. R. and Zhuang, X.: Image analysis using mathematical morphology, *IEEE Transactions on Pattern Analysis and Machine Intelligence*, PAMI-9,(4): 532–550, 1987.
- Koistinen, J.: Bird migration patterns on weather radars, 1st European Conference on Radar Meteorology, Bologna, Italy, Vol. 25 of *Physics and Chemistry of the Earth (Part B: Hydrology, Oceans and Athmosphere)*, European Geophysical Society, Pergamon Press, pp. 1185–1193, 2000.
- Peura, M., Koistinen, J. and King, R.: Visual modelling of radar images, COST-75: *Advanced weather radar systems – international seminar*, European Commission, pp. 307–317, 1998.
- Sonka, M., Hlavac, V. and Boyle, R.: *Image Processing, Analysis and Computer Vision*, Chapman & Hall Computing, 1993.